Biophysical Journal
Article

Biophysical Society

Mechanical control of cell proliferation patterns in growing epithelial monolayers

Logan C. Carpenter,[1] Fernanda Pérez-Verdugo,[1] and Shiladitya Banerjee[1,*]
[1]Department of Physics, Carnegie Mellon University, Pittsburgh, Pennsylvania

ABSTRACT Cell proliferation plays a crucial role in regulating tissue homeostasis and development. However, our understanding of how cell proliferation is controlled in densely packed tissues is limited. Here we develop a computational framework to predict the patterns of cell proliferation in growing epithelial tissues, connecting single-cell behaviors and cell-cell interactions to tissue-level growth. Our model incorporates probabilistic rules governing cell growth, division, and elimination, also taking into account their feedback with tissue mechanics. In particular, cell growth is suppressed and apoptosis is enhanced in regions of high cell density. With these rules and model parameters calibrated using experimental data for epithelial monolayers, we predict how tissue confinement influences cell size and proliferation dynamics and how single-cell physical properties influence the spatiotemporal patterns of tissue growth. In this model, mechanical feedback between tissue confinement and cell growth leads to enhanced cell proliferation at tissue boundaries, whereas cell growth in the bulk is arrested, recapitulating experimental observations in epithelial tissues. By tuning cellular elasticity and contact inhibition of proliferation we can regulate the emergent patterns of cell proliferation, ranging from uniform growth at low contact inhibition to localized growth at higher contact inhibition. We show that the cell size threshold at G1/S transition governs the homeostatic cell density and tissue turnover rate, whereas the mechanical state of the tissue governs the dynamics of tissue growth. In particular, we find that the cellular parameters affecting tissue pressure play a significant role in determining the overall growth rate. Our computational study thus underscores the impact of cell mechanical properties on the spatiotemporal patterns of cell proliferation in growing epithelial tissues.

SIGNIFICANCE Control of cell proliferation in multicellular environments is crucial for tissue development and homeostasis. To understand the regulation of cell proliferation, we developed a multi-layered computational model that integrates physical interactions between cells with active cell behaviors governing cell fate decisions. Using this model, we investigated the impact of cellular crowding on cell size control, growth rate, and division dynamics. The multi-scale model enabled us to elucidate the role of single-cell properties in determining epithelial tissue homeostasis, growth kinetics, and spatial patterns of proliferation. Notably, we found that cellular elasticity and contact inhibition of proliferation governed the emergent dynamics of cell proliferation, emphasizing the impact of cellular mechanics on cell proliferation dynamics in epithelial tissues.

INTRODUCTION

The regulation of cell proliferation is critical for tissue development, maintenance of homeostasis, and disease suppression (1,2). Uncontrolled proliferation results in hyperplasia, a hallmark of cancerous mutations (3). Cell proliferation involves the coordinated processes of cell growth and division at the individual cell level. However, the precise coordination of cell growth and division within the multicellular context is still poorly understood. One mechanism implicated in the control of cell growth is contact inhibition of proliferation, where cellular growth is inhibited in denser environments (4). In epithelial tissues, contact inhibition has been shown to be regulated by several factors, including intercellular signaling (5–7), cellular crowding (8,9) mechanical stress (10–12), and pressure (13). In particular, cells under compression grow slower than cells under stretch (10,14). However, cellular response to mechanical stress and intercellular signaling is influenced by various factors, such as cell-cell adhesion, cellular resistance to deformations, cytoskeletal tension, local cell density, and cell-cycle phase. Manipulating these factors individually within tissues is challenging, leaving the

Submitted July 26, 2023, and accepted for publication March 1, 2024.
*Correspondence: shiladtb@andrew.cmu.edu
Editor: Jennifer Schwarz.
https://doi.org/10.1016/j.bpj.2024.03.002

relative contributions of mechanical and biochemical processes in regulating cell growth largely unexplored.

Cell proliferation relies crucially on the mechanism of cell division. Although cell growth and division are coupled in single cells (15,16), cell division can occur independently of growth in tissues (17). Various models of cell division control have been proposed in recent years for bacteria and eukaryotes, as reviewed in Refs. (15,18). These include the adder model (19–21), where cells grow by a fixed volume between successive divisions; the sizer model (22,23), where cell division occurs above a critical cell size threshold (8,24); as well as mixed models of cell size control (25,26). Recent studies on mammalian epithelial cells, however, suggested that the regulation of the cell cycle in both single cells and tissues can be well described by a G1 sizer model (26,27). In this model, there is a cell-size-dependent transition from the growth (G1) phase to the mitosis (S/G2/M) phase. Cells spend a fixed amount of time in S/G2/M phase before division occurs. Consequently, the rate of cell division is regulated by the time required to reach the critical size threshold at the G1/S transition, which, in turn, depends on cellular growth rate. Considering the diverse range of biophysical factors influencing cell size and growth rate, it remains to be determined how cell proliferation patterns in tissues are precisely controlled by these factors.

Many cell-based models of epithelial tissue growth have been developed in recent years, which explored the effects of contact inhibition (28–30), cellular crowding (9,31), mechanical stress (8,10,11), and intercellular adhesion (32) on tissue-scale growth dynamics. In particular, it has been observed that contact inhibition of proliferation leads to enhanced cell proliferation at tissue boundaries while inhibiting growth within the bulk of the tissue (8,10). Notably, experiments have revealed diverse patterns of tissue growth, including bulk epithelial growth in vitro (27,33) and in vivo (34), as well as spatially patterned growth in vitro (33,35). How the emergent patterns of cell proliferation are regulated by cell-cell mechanical interactions remains unclear.

In this work, we developed a cell-based model for epithelial monolayer growth that aims to uncover how single-cell behaviors and mechanical properties govern tissue-scale proliferation patterns. Our integrative model couples the physical dynamics of cells with active cellular behaviors that determine their fates (Fig. 1). The physical layer of the model is implemented using the cellular Potts model (36), whereas the active behaviors are implemented as rules for cell-cycle regulation, contact inhibition of proliferation, and cell elimination via apoptosis and extrusion. In contrast to previous cellular models for tissue growth (8,10,30,31,37,38), we incorporate a G1 sizer model for cell-cycle progression (27) that allows for tunable growth rates of individual cells based on the amount of crowding. Furthermore, our model implements contact inhibition through crowding-induced suppression of cellular growth

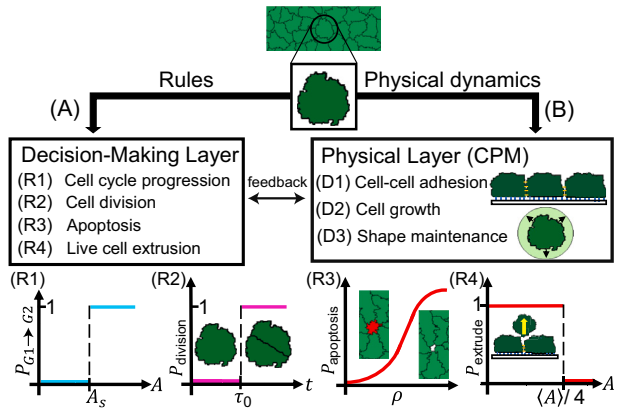

FIGURE 1 Overview of the computational modeling framework. (*A*) Cell-autonomous decisions and their rules. (*R1*) Cycle progression from G1 (sizer phase) to S/G2/M (timer phase) phase is triggered by the cell area exceeding a threshold value A_S. (*R2*) Mitosis is triggered after a time τ_0 has elapsed since the beginning of the S/G2/M phase. (*R3*) Apoptosis is triggered probabilistically as a function of local cell density. (*R4*) Cellular extrusion is triggered when the cell area reaches one fourth of the mean area for all cells in the tissue. (*B*) The physical layer evolves via probabilistic minimization of cell mechanical energy using the cellular Potts model, which accounts for (*D1*) contact energy at cell-cell and cell-medium interfaces, (*D2*) growth in cell size by increasing cell target area and subsequent relaxation of area elastic energy, and (*D3*) cell shape maintenance by relaxing mechanical energy of the cell. To see this figure in color, go online.

rate and introduces a cell-density-dependent probability of apoptosis. Taken together, our model incorporates feedback between mechanical pressure and the rates of cell growth, division, and apoptosis within a tissue context.

Using this model, we successfully recapitulated several single-cell behaviors observed experimentally, including the distribution of cell areas, the control of cell-cycle duration, and the decrease in cell size over time. The latter is caused by a transition from a sizer-like to a timer-like control of cell size that leads to volume-reductive cell division as local cell density is increased via tissue growth. Subsequently, cell-cycle arrest occurs as cell size falls below the minimal size threshold required for G1/S transition. Notably, we found that the cell size threshold at the G1/S transition is the primary determinant of tissue properties in homeostasis, including homeostatic density and steady-state rates of cell division and elimination. In contrast, the rate of cell proliferation is predominantly regulated by the physical properties of cells, specifically cell elasticity, growth rate, and sensitivity to contact inhibition. Interestingly, spatial patterns of cell growth and cell cycle exhibit variations depending on the values of cell elastic modulus and sensitivity to contact inhibition. Tissues with moderate to high sensitivities to contact inhibition display boundary growth, whereas tissues with a higher cell elastic modulus exhibit bulk growth. For intermediate values of elastic modulus and contact inhibition, diverse patterns of cell proliferation emerge, emphasizing the influential role of

TABLE 1 Default Parameters Used in Model Simulations

Parameter	Numerical Value (units)	Description
k_BT	$1.95 \times 10^{-4}(\lambda A_S^2)$	thermal energy scale of Metropolis-Hastings algorithm
J_{cc}	$1.17 \times 10^{-4}(\lambda A_S^{3/2})$	cell-cell contact energy
J_{cm}	$1.96 \times 10^{-4}(\lambda A_S^{3/2})$	cell-medium contact energy
λ	1	cell-area elastic modulus
G	$1.16\ (A_{S_0}/\tau_0)$	growth rate of an isolated cell
k	$1.897 \times 10^5\ (A_S^{-2})$	sensitivity to crowding
τ_0	225 ± 5.625 (Monte Carlo steps)	S/G2/M timer duration
A_S	1377 ± 34.4 (pixels)	G1 sizer threshold
$p_{apo,max}$	0.0015	maximal probability of apoptosis
$\rho_{1/2}$	$1.5015\ (A_S^{-1})$	cell density at half-maximal probability of apoptosis
α	$0.968\ (A_S)$	sensitivity to density-dependent apoptosis

mechanical factors in governing tissue-scale proliferation dynamics. These findings provide new insights into the intricate interplay between mechanical and cellular factors in tissue growth regulation.

MATERIALS AND METHODS

Computational model

To predict the emergent patterns of cell proliferation, we developed a two-dimensional cell-based model for epithelial monolayer tissue growth that integrates two distinct computational layers: 1) a physical layer that simulates mechanical interactions between cells and between cells and the external medium; and 2) a decision-making layer that encodes cell-autonomous rules for growth, division, and apoptosis (Fig. 1). For simplicity, we neglected cell motility and focused on the role of cell mechanics and cell-cycle regulation on tissue growth.

In the physical layer, we used the lattice-based cellular Potts model (36,39) at a finite temperature, where cells are formed by a subset of lattice sites sharing the same identity. Each lattice site i is assigned a type $\sigma_i = \{\mathrm{c} : \mathrm{cell}, \mathrm{m} : \mathrm{medium}\}$ and an integer-valued identity n_i, with $n_i = 0$ for the external medium and $n_i > 0$ for a cell. The mechanical energy of cells in the cellular Potts model can be written in a simplified form as

$$E = \sum_{\substack{i,j \\ \text{neighbors}}} J_{ij}(\sigma_i, \sigma_j) + \lambda \sum_{\alpha \in \text{cells}} b\left(A_\alpha - A_\alpha^T\right)^2, \qquad \text{(Equation 1)}$$

where the first term represents interfacial energy arising from tension at cell-cell junctions, adhesion between cells, and between cells and the extracellular medium. The interfacial energy is summed over adjacent lattice sites i and j, with $n_i \neq n_j$. The energy J_{ij} can take two different values depending on the adjacent lattice types: $J_{ij}(\mathrm{c},\mathrm{c}) = J_{cc}$ and $J_{ij}(\mathrm{c},\mathrm{m}) = J_{ij}(\mathrm{m},\mathrm{c}) = J_{cm}$. We assumed greater adhesion for cell-cell contact than cell-medium contact yielding the condition $J_{cc} \leq J_{cm}$. The second energy term is summed over all the cells, representing an elastic energy that penalizes deviations of the cell areas A_α from their preferred (target) values A_α^T, with an area elastic modulus λ. At each computational time step, the lattice site i can take the value of its adjacent site n_j (with $n_i \neq n_j$), inducing cell shape changes. These lattice moves are executed via the Metropolis-Hastings algorithm (40,41) to ensure that the moves minimize the mechanical energy.

The decision-making layer implements cell-autonomous rules for cell-cycle progression, mitosis, apoptosis, extrusion, and changing the cell's target area. Cell growth is implemented by increasing the cell's target area A_α^T (31), as

$$\frac{dA_\alpha^T}{dt} = Ge^{-k\left(A_\alpha - A_\alpha^T\right)^2}, \qquad \text{(Equation 2)}$$

where the constant G represents the rate of growth in the absence of crowding (when $A_\alpha \sim A_\alpha^T$). We define k as a metric of cellular sensitivity to crowding. In crowded conditions, it is difficult for cells to maintain their areas close to the growing target area, and hence $\Delta A_\alpha = A_\alpha - A_\alpha^T$ increases in magnitude. Under these conditions, Eq. 2 leads to an exponential decay in the rate of cell growth, resulting in longer cell-cycle times proportional to k. Contact inhibition in our model is thus a consequence of physical constraint induced by tissue crowding (8), resulting in deviation of cell area from its preferred value in isolation (27).

The number of cells in the tissue, N, changes in time due to the rules implemented in the decision-making layer. N can increase through cell divisions, which is regulated by a G1 sizer model (26,27). In this model, a cell is in the G1 phase until its area is greater than a threshold value A_S (Fig. 1 *A*–R1), at which point it transitions to the S/G2/M phase, which lasts for a fixed time period τ_0 (a timer). After a time τ_0 in the S/G2/M phase, the cell divides into two cells (Fig. 1 *A*–R2), upon which the target area of each cell is set to the current area. Both τ_0 and A_S are drawn from a Gaussian distribution, with mean and standard deviation defined in Table 1, based on data reported for Madin-Darby canine kidney (MDCK) cells (27).

On the other hand, the number of cells in the tissue can decrease via cellular apoptosis and extrusion. The model considers a density-dependent probability of apoptosis, P_{apo}, which increases with the local cell density ρ (9,42,43) (Fig. 1 *A*–R3)

$$P_{apo}(\rho) = \frac{p_{apo,max}}{1 + e^{-\alpha\left(\rho - \rho_{1/2}\right)}}, \qquad \text{(Equation 3)}$$

where $p_{apo,max}$ is the maximal probability of apoptosis, $\rho_{1/2}$ is the cell density at half-maximal probability, and α is the sensitivity to density-dependent apoptosis. The parameters $p_{apo,max}$, $\rho_{1/2}$ and α are determined by fitting apoptosis probabilities calculated from in vitro MDCK cell competition experiments performed by Bove et al. (9). In our simulations, local cell density was defined as the sum of inverse cell areas within the immediate neighborhood of a given cell α (9,31),

$$\rho_\alpha = \frac{1}{A_\alpha} + \sum_{i \in \text{ neighbors of } \alpha} \frac{1}{A_i}, \qquad \text{(Equation 4)}$$

where we defined local neighborhood as the set of first neighbors of a cell (i.e., all the cells in physical contact with a given cell). After entering apoptosis, the cell's target area is set to zero, causing the cell to gradually decrease in area until being removed. Finally, a cell is eliminated via live-cell extrusion if its area is less than a quarter of the mean cellular area (i.e., $A_\alpha \langle A_\alpha \rangle / 4$; Fig. 1 *A*–R4). This is handled computationally by immediately

deleting the cell, which reassigns the deleted cell's lattice sites to medium lattice sites. Taken together, the rate of cell proliferation in the tissue is given by $\dot{N} = k_{\text{birth}} - k_{\text{elim}}$, where k_{birth} corresponds to the rate of cellular divisions and k_{elim} corresponds to the rate of cell elimination via both apoptosis and extrusion. Combining the physical and decision-making layers results in a predictive cell-based model (see supporting material for details) that can simulate the spatiotemporal dynamics of a growing tissue in different biophysical contexts.

RESULTS AND DISCUSSION

Collective behaviors in growing epithelial monolayers

To validate the predictive capacity of our model, we used it to recapitulate experimentally observed collective and single-cell behaviors in growing epithelial monolayers (8, 27). We simulated the growth of a planar epithelial tissue, confined within a square box of area $\sim 1600A_S$ (Videos S1 and S2). The simulations were initialized with a single cell of area below the G1 sizer threshold A_S. As a first step, we performed two ensembles of simulations: 1) tissue growth without apoptosis ($P_{\text{apo}} = 0$, Video S1), and 2) tissue growth with apoptosis, occurring with a density-dependent probability P_{apo} as defined in Eq. 3 (Video S2). Here, we considered the limit in which the scale of the elastic force, $\lambda A_S^{3/2}$, is larger than the tension between cells, J_{cc}, and the tension between boundary cells and the external medium, J_{cm}, with $J_{cm} > J_{cc}$ (see Table 1 for a list of default parameter values). Consequently, the tissues grew while maintaining their initial isotropic state, with a roughly circular boundary, until they made contact with the simulation box (Fig. 2 *E* and *F*; Videos S1 and S2).

Our model accurately captured the experimentally measured trends in the dynamics of cell count and average cell density during epithelial colony growth and homeostasis (Figs. 2 *A* and *B* and S8) (9). During the growth phase of the tissue, constituent cells exhibited nonuniform sizes and growth rates, with a slowly growing bulk region surrounded by a rapidly proliferating periphery (Fig. 2 *E* and *F*). Rapid replication of cells near the boundary have previously been observed in several experiments on epithelial tissues (8,10,13,33). In our model, this results from crowding-induced suppression of growth in the bulk of the tissue, which results in smaller cell size in the bulk compared to the periphery (Fig. 2 *C* and *D*). With or without apoptosis, the simulated tissues grew until they reached confluence, filling the entire simulation box (Fig. 2 *E* and *F*). This was followed by a state of homeostasis where the cell count and the average density did not change. In this state, the rates of cell division and elimination balanced to yield a net zero growth rate. Confluence led to uniform crowding throughout the tissue, resulting in the homogenization of the cellular areas and density (Fig. 2 *A* and *B*).

In simulations without apoptosis, the rate of cell elimination k_{elim} arises from live-cell extrusions only. Homeostasis in these simulations is characterized by $k_{\text{birth}} = k_{\text{elim}} = 0$, where all the cells are arrested in the G1 phase, with $A_\alpha < A_S$, $\forall\, \alpha$. By contrast, in simulations with apoptosis, the elimination rate is dependent on both live-cell extrusions and apoptosis, the latter being a density-dependent probabilistic process. Therefore, homeostasis is characterized by a dynamic balance between birth and elimination, with $k_{\text{birth}} = k_{\text{elim}} \neq 0$. Cell density-dependent apoptosis events induced cellular growth in the neighborhood of a dying cell (Fig. 2 *F*), leading to increased cell size and lower values of cell count and average cell density (Fig. 2 *A* and *B*). Furthermore, cell elimination events increased the time required to reach homeostasis (Fig. 2 *A*), promoting continuous cell turnover and growth in the tissue.

Single-cell dynamics underlying epithelial growth and homeostasis

Spatial regulation of cell proliferation is a direct consequence of how cell cycle and growth are regulated across a tissue (Figs. 2 *E* and *F* and S1). Here, we characterize the single-cell growth and size dynamics underlying the growth of an epithelial colony. A major regulator of single-cell growth rate is local crowding by other cells. Growth rate of cells in the bulk of the tissue reduced over time due to an increase in local cell density, leading to a transition in the mitotic behavior of cells. During the early phase of growth (up to $t \approx 7\tau_0$), cells exhibited timer-like behavior with divisions occurring at regular intervals of τ_0 due to the cell size being larger than the G1 sizer threshold A_S (Fig. 3 *A*). During this period, cell size distribution was unimodal (Fig. 3 *C* and *D*), with a mean value $\overline{A} > A_S$. Mean cell area, $\overline{A}$, decreased in time since the amount of growth accrued in the timer (S/G2/M) phase, $G\tau_0 \sim 1.16A_S < \overline{A}$, was less than the amount of cell size reduction via division. This phenomenon of size-reductive divisions recapitulates experimental observations in growing MDCK monolayers (8,27).

Once cell size in the population fell below A_S (Fig. 3 *C* and *D*, $t > 7\tau_0$), two sub-population of cells emerged: one with mean size above A_S that would divide after time τ_0 in the G2 phase, and another with mean size below A_S that would be growing in the G1 phase and therefore would divide in a time longer than τ_0. This behavior is evident in the cell area distribution, which changed from a unimodal to a bimodal shape (see $t \sim 7.6\tau_0$ in Fig. 3 *C* and *D*). However, as cell crowding increased via an increase in the local cell density (Fig. 3 *A* and *B*), cell area decreased over several generations, narrowing the area distribution (Fig. 3 *C* and *D*). A consequence of crowding-induced slowdown of single-cell growth is a negative correlation between cell area and interdivision time (Fig. 3 *E* and *F*), as observed experimentally (8).

In our analysis, the onset of confluence is defined as the time at which 99.5% of the simulated space is occupied by cells within the tissue. Post confluence ($t > 35\tau_0$), cell growth

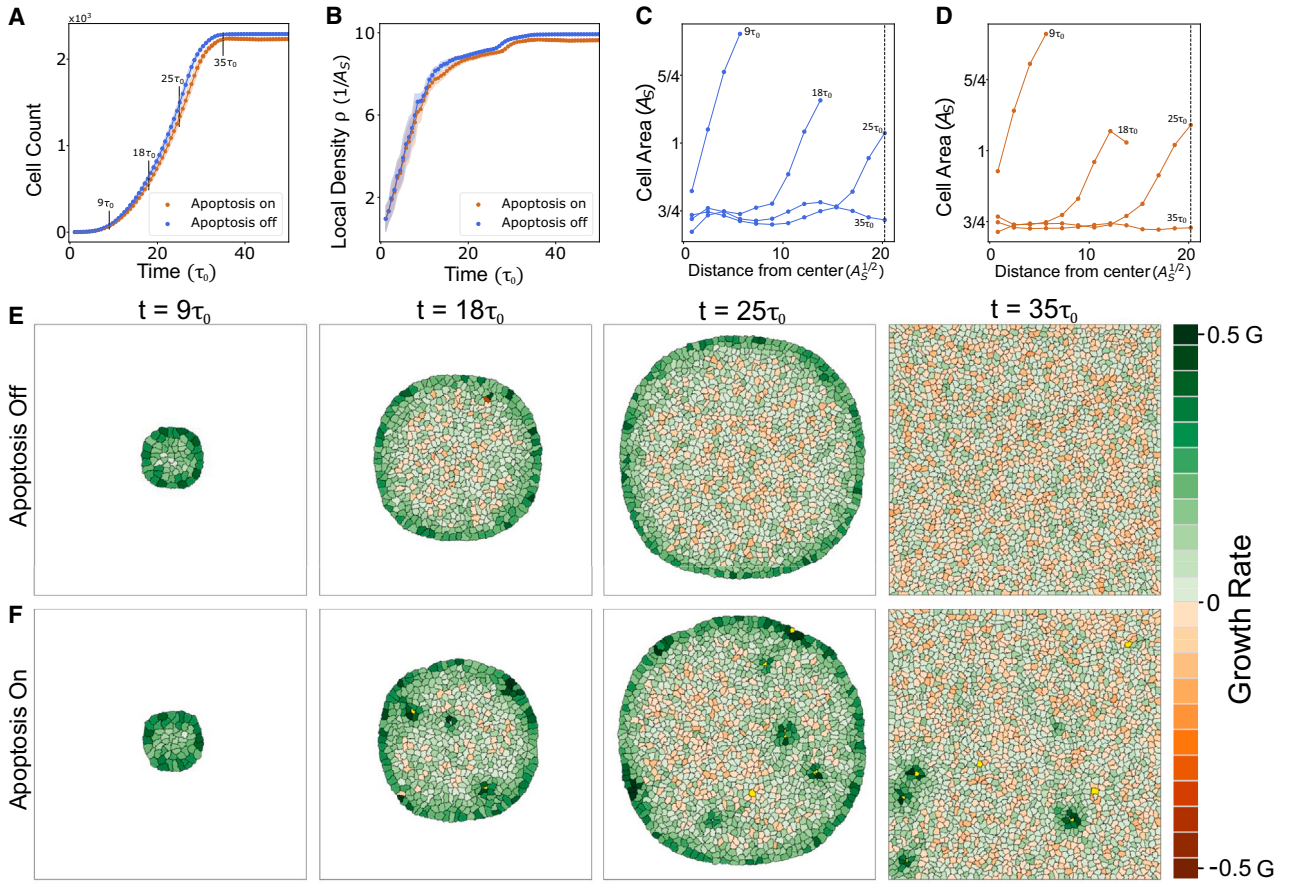

FIGURE 2 Characterization of collective behaviors in growing epithelial monolayers. (*A* and *B*) Cell count vs. time (*A*) and average cell density vs. time (*B*) in colony growth simulations with apoptosis on (*orange*) and off (*blue*). The x axis represents time measured in factors of τ_0, the mean timer threshold. (*C* and *D*) Spatial distribution of single-cell areas for monolayers at different time points during growth, without (*C*) or with (*D*) apoptosis. Each curve represents a colony's spatially averaged cell area as a function of distance from the center of the colony. The vertical dashed line is position of the boundary of the simulation box. In (*A*)–(*D*), each data point is the average of five simulations with the shaded regions being the standard deviation. (*E* and *F*) Time-lapse showing the morphologies of a growing epithelial colony without (*E*) or with (*F*) apoptosis. Cells are colored according to their growth rates. See Table 1 for a list of parameter values. To see this figure in color, go online.

was either nonexistent or slow due to the lack of available free space. In simulations without apoptosis, cells underwent complete cycle arrest (Fig. 3 *A*), as a result of the lack of tissue turnover to free up space. By contrast, in simulations with apoptosis, the rates of growth and division were limited by the available free space that appears after cell elimination. Consequently, the cell cycles progressed at a very slow rate ($t \geq 20\tau_0$ in Fig. 3 *B*), primarily determined by the rate of apoptosis within the tissue. These slowly growing cells were stuck in the G1 phase for the majority of the cell cycle and divided relatively fast after exceeding the G1 size threshold A_S, thereby exhibiting sizer-like behavior.

G1 sizer sets homeostatic cell density and turnover rate

Having validated our model predictions for collective and single-cell behaviors against experimental observations, we turned to assessing the roles of cell-scale parameters on the emergent tissue-level properties during growth and homeostasis. To this end, we varied the model parameters regulating cell growth and division dynamics, including the growth rate G, area elastic modulus λ, cell-cell adhesion energy J_{cc}, sensitivity to crowding k, and the G1 sizer threshold A_S. As a first step, we studied the effect of these parameters on homeostatic tissue properties, including homeostatic cell density and turnover rate.

Prior studies have demonstrated that epithelial tissues possess a specific density they tend to restore after perturbations, indicating their tendency to maintain a preferred homeostatic density (14,44,45). However, the mechanisms underlying the regulation of this homeostatic density, which plays a pivotal role in maintaining tissue homeostasis (14,43,46) and cell competition (31,42), remain poorly understood. Our simulations revealed that the G1 sizer threshold A_S is the only parameter that determines the homeostatic density (Fig. 4 *A* and *C*). This can be intuitively understood from the fact that A_S regulates cell size limit

SUPPLEMENTAL METHODS

Cellular Potts Model

We used the Cellular Potts Model (CPM) [1] to simulate the dynamics of a growing tissue. Although alternative cell-based modeling frameworks exist for tissue modeling, such as vertex models [2], cell-center models [3], or particle-based models [4], our choice of CPM was motivated by its ease of implementation for key aspects of this study, including straightforward integration of agent-based rules, boundary conditions, and interactions between cells and the extracellular medium. Our simulation framework integrates two distinct computational components: (1) a physical layer that simulates cell mechanics with the Cellular Potts Model, and (2) a decision-making layer that defines rules for cell growth, division, and apoptosis. The CPM is a versatile computational framework for simulating biological systems such as cell growth, migration, and tissue formation. The CPM runs a Monte Carlo simulation with the Metropolis-Hastings algorithm [5, 6] to minimize the free energy of the system.

A common choice of the Hamiltonian [1] includes terms that represent contact energies and an area elastic energy, as in

$$E = \sum_{\substack{i,j \\ \text{neighbors}}} J_{ij}(\sigma_i, \sigma_j) + \lambda \sum_{\alpha \in \text{cells}} \left(A_\alpha - A_\alpha^T\right)^2 , \tag{S.1}$$

The contact energy, $J_{i,j}$, is given by the difference between the cellular surface tension and intercellular adhesion energy. This energy is represented in the Hamiltonian by a component that is proportional to the number of pixels shared between cells or between a cell and the medium. The sum goes over all adjacent lattice sites i and j, ignoring self-adhesion. The inner term, σ, gives the cell type at the lattice site i and j respectively. A value for contact energy is defined between each cell type, which for our simulations consists of interactions between cells and medium $J_{\text{cell-cell}} = J_{\text{cc}}$, $J_{\text{cell-medium}} = J_{\text{cm}}$, and $J_{\text{medium-medium}} = J_{\text{mm}}$. The second term in the Hamiltonian is the area elastic energy. This is given by the product of the area elastic modulus, λ, with the sum of squared differences between the actual area of the cells, A_α, and their target areas, A_α^T. These two mechanical energy components regulate individual cell shape and size, in the absence of other rules.

The CPM simulations were run using CompuCell3D [7], a software package that handles all of the computations necessary for the CPM and the Metropolis-Hastings algorithm. The version of CompuCell3D we used permits cell fragmentation proportional to the lattice temperature, which we set $T = 10$ in the units of lattice energy. We found that this temperature produced negligible fragmentation.

Rules for active cell behaviors

The decision-making layer of the model encodes probabilistic rules for active cell behaviors including changes in cell target area, cell cycle regulation, and cell elimination.

Dynamics of cell growth – Cell growth dynamics are implemented by increasing the cell's target area as

$$\frac{\mathrm{d}A_\alpha^T}{\mathrm{d}t} = Ge^{-k(A_\alpha - A_\alpha^T)^2}, \tag{S.2}$$

where G is the growth rate in the absence of crowding, k quantifies cellular sensitivity to crowding, and A_α is the current area of cell α. In the presence of crowding, a cell's area will deviate from its target area, and this deviation is directly proportional to the strength of contact inhibition. Consequently, cellular growth exhibits an exponential decline as crowding intensifies, ultimately leading the tissue to enter an arrested state.

Cell cycle regulation – We implemented a two-phase cell cycle model, comprising a G1 growth phase operating through a sizer mechanism, followed by an S/G2/M timer phase. When a cell is born, it is assigned a G1 area threshold A_S and an S/G2/M phase timer τ. The cell remains in the G1 phase until its area exceeds A_S. Afterward, it enters the S/G2/M phase, which lasts for a duration of τ. Since the S/G2/M phases are grouped into the singular timer phase, we decided to make the change in target area (eq S.2) independent of the cell cycle phase. The assumption of continuous growth through the cell cycle is informed by growth data on single epithelial cells [8]. Upon completion of the S/G2/M phase, the cell immediately undergoes division, perpendicular to the semi-major axis, resulting in two daughter cells, both of which enter the G1 phase.

Mechanisms for cell elimination – In the simulation, cell elimination involves two mechanisms: programmed cell death (apoptosis) and live-cell extrusion. Experimental data have shown that increasing cell density leads to a higher apoptosis rate [9–11]. We defined the local cellular density as the sum of inverse cell areas within a local neighborhood of a cell. The density of cell α is given by:

$$\rho_\alpha = \frac{1}{A_\alpha} + \sum_{i \in \text{neighbors of } \alpha} \frac{1}{A_i}. \tag{S.3}$$

To model the probability of apoptosis in wild-type MDCK cells as a function of local cell density [11], we fit the data to a sigmoid curve:

$$P_{\text{apo}}(\rho) = \frac{p_{\text{apo,max}}}{1 + e^{-\alpha(\rho - \rho_{1/2})}}. \tag{S.4}$$

In the simulations, the probability of apoptosis is calculated every 10 Monte Carlo steps, which, on the time scale of the timer threshold, reproduces the experimentally observed probabilities. When a cell is eliminated

through apoptosis, its target area is set to zero, causing it to shrink rapidly. During this process, surrounding cells grow to occupy the space left by the apoptotic cell. Within the simulation, this is implemented as:

1. Loop over every cell

    (a) Calculate the local density, ρ_c (eq S.3), for a cell.

    (b) Check if the cell dies with probability $P(\rho_c)$ (eq S.4)

        i. If the cell dies the target area and elastic modulus are set to $A_T = 0$ and $\lambda = 5$ in order to encourage rapid (but not instantaneous) shrinking of the dying cell.

In addition to apoptosis, cells can also be eliminated via live cell extrusions. This occurs when a cell's area significantly decreases compared to the average population area. In experiments [9], extrusion happens when tissue experiences compressive stress, causing a cell to delaminate from the substrate and eject from the monolayer. In our simulations, a cell whose area falls below $\langle A \rangle/4$ (where $\langle A \rangle$ is the average area of the colony) is immediately removed to capture the short time scale over which extrusion occurs [9, 12]. Within the simulation, this is implemented as:

1. Calculate the average cellular area, $\langle A \rangle$, within the tissue.

2. Loop over every cell to see if a cell's area, A_c, satisfies $A_c < \langle A \rangle/4$.

    (a) Each cell whose area satisfies the above condition is immediately ejected. This is done by converting each lattice site the cell occupied into medium sites.

Choice of Default Model Parameters

Converting lattice units in the CPM framework to physical units is essential for comparing our simulations with experimental observations. There are two key conversions: translating pixels and Monte Carlo Steps (mcs) into SI units for distance and time. To achieve this, we compared the experimentally reported values for average cell volume during subconfluence for MDCK cells [8, 13, 14] with the value for average subconfluent colony area in our simulations, $\bar{A}_{SC} = 3200$ pixels. This comparison yielded the conversion factor: 1 pixel $= (0.13 \pm 0.03)\mu m^2$. Applying this factor to the G1/S size threshold, we obtained $A_S = 1377$ pixels $= (179.01 \pm 41.31)\mu m^2$. We normalized simulation time with the average cycle time of an uncrowded cell, i.e., the cell's timer duration τ_0. Experimental data for typical epithelial cell types suggest that the time

for the S/G2/M phase is approximately $\tau_0 \approx 10$ hours [8, 14]. This provides the timescale conversion from Monte Carlo steps to hours, $\tau_0 = 225$ mcs ≈ 10 hr (or 1 mcs ≈ 2.67 min).

The single-cell growth rate G is sampled from a Gaussian distribution to determine the change in the target area at each Monte Carlo step (Eq. (S.2)). The mean value of G is set such that isolated cells maintain the average subconfluent area $\bar{A}_{SC}$, $G_0 = \frac{1}{2}\frac{\bar{A}_{SC}}{\tau_0}$, and the standard deviation is set to $0.05\ G_0$. While G sets cellular growth rate ($\mathrm{d}A^T/\mathrm{d}t$) in an isolated state, tissue crowding reduces the available space for growth to bulk cells, causing their actual area to deviate from the target area. This results in the domination of the exponential term of Eq. (S.2), $e^{-k(A-A^T)^2}$, and drives the growth $\mathrm{d}A^T/\mathrm{d}t$ to zero until the cell's area increases. The sensitivity to crowding, represented by the heuristic parameter k, quantifies the allowable deviation between a cell's area and its target area. The default value, $k = 0.1$ pixels^{-2}, was determined empirically to ensure the tissue growth rate captures the expected growth dynamics over several cell cycles.

In our implementation of the CPM, there are four parameters within the Hamiltonian that set the energy scale; elastic energy has λ and contact energy has J_{cc}, J_{cm}, and J_{mm}. The parameter λ represents the area elastic modulus for the cell, and we choose a default value $\lambda = 1$. The parameter J represents the disparity between cell surface tension and intercellular adhesion, implying that higher J values indicate lower cell-cell adhesion. Consequently, we chose $J_{\mathrm{cc}} = 6$ and $J_{\mathrm{cm}} = J_{\mathrm{mm}} = 10$, which allowed cells to adhere more strongly to each other than the medium, resulting in a circular morphology for the growing colony.

Video Legends

Video S1. Simulation of a growing epithelial colony with apoptosis turned off. The simulation uses default parameters as listed in Table 1. Individual cells are color coded by their growth rates.

Video S2. Simulation of a growing epithelial colony with apoptosis turned on. The simulation uses default parameters as listed in Table 1. Individual cells are color coded by their growth rates. Dying cells are colored yellow to highlight them within the tissue.

Video S3. Simulation of a growing epithelial colony exhibiting boundary growth due to strong contact inhibition. The simulation uses default parameters as listed in Table 1, except elastic modulus $\lambda = 1$ and sensitivity to crowding $k = 1$. Left: Cells are color coded by their growth rates, Right: Cells are color-coded by the cell cycle phase (blue: G1 phase, fuchsia: S/G2/M phase).

Video S4. Simulation of a growing epithelial colony exhibiting uniform bulk growth due to weak contact